Rheology of a Comblike Liquid Crystalline Polymer as a Function of Its Molecular Weight

V. Fourmaux-Demange,*,† A. Brûlet,† J. P. Cotton,† L. Hilliou,‡ P. Martinoty,‡ P. Keller,§ and F. Boué†

Laboratoire Léon Brillouin (CEA-CNRS), CEA Saclay, F91191 Gif/Yvette, France, Laboratoire d'Ultrasons et de Dynamique des Fluides Complexes, ULP, 4 rue Blaise Pascal, F67070 Strasbourg, France, and Section de Recherche, Institut Curie, F75231 Paris Cedex 05, France

Received September 26, 1997; Revised Manuscript Received March 9, 1998

ABSTRACT: We have performed rheological studies on a nonentangled comblike liquid crystalline polymer. Fractionated samples of six different molecular weights and a nonfractionated sample (large molecular weight distribution) were studied. The storage and loss moduli, G' and G'', were measured as a function of frequency for different temperatures, in the isotropic phase for the fractionated samples and in both isotropic and nematic phases for the nonfractionated one. They were found to obey time/temperature superposition in both phases. At intermediate frequencies, G' and G'' obeyed a frequency power law: $G' \sim G'' \sim \omega^{0.6}$. At low frequencies in the isotropic phase, the zero-shear rate viscosity, η_0, and an average terminal time, τ_{ter}, were measured as a function of molecular weight. The power laws obtained are: $\eta_0 \sim M_w^{1.3 \pm 0.1}$ and $\tau_{ter} \sim M_w^{2.6 \pm 0.3}$. These results are discussed in the frame of the classical Rouse model for free chains. Possible effects of interactions between the teeth of the combs are also considered.

Introduction

Comblike liquid crystalline (CLLC) polymers[1] consist of linear chains with a rigid mesogenic group grafted as a side chain through a flexible spacer on each monomer. In the molten state, these polymers present, as temperature varies, the characteristic phases of liquid crystals (nematic, smectic). The ability of quenching an oriented state on cooling below the glass temperature (T_g) makes them interesting for industrial applications.[2]

The study of their dynamics in the nematic phase gives rise to a fundamental question: What is the influence of the long-range liquid crystalline interaction on the polymeric dynamics? Most of the rheological studies reported[3,4] seem to show that the nematic order plays no role in the dynamics of the chains: viscoelastic properties are qualitatively similar in the isotropic (I) and nematic (N) phases. The main effect of the nematic interaction is to increase viscosity and relaxation times in a continuous way through the IN transition. This is fundamentally different from main-chain liquid crystalline polymers for which viscosity drops upon transition to nematic state.[5] However, some specific differences exist between this comblike polymer and linear polymers. We will focus on them below.

A first study of the relaxation after deformation of a CLLC polymer using small angle neutron scattering (SANS) was undertaken.[6] This technique allows selective probing of the backbone dynamics. Thus the contribution of the polymer backbone to viscoelasticity can be separated from that of the nematic interaction. The polymer chosen was a polymethacrylate, called PMA−CH_3, with a side branch consisting of a spacer of six carbons, phenyl moieties, and a methyl terminal group. Its chemical formula is

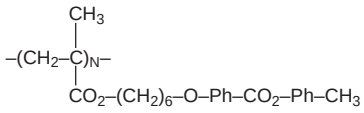

where N is the degree of polymerization.

This polymer is particularly interesting since it shows a nematic phase on a large range of temperature (ranging from 44 to 83 °C). It is therefore possible to study its properties in the nematic phase as a function of temperature. This advantage will be very useful for neutron studies,[7] but for experimental reasons, the nematic phase is scarcely studied in this work.

Preliminary neutron scattering experiments[8] on nondeformed samples showed that the backbone of PMA−CH_3 in the isotropic phase had the same conformation as an usual linear flexible polymer, the polystyrene (PS). Thus, in the isotropic phase, the conformation is that of a random coil. On the contrary, the dynamic aspect revealed quasi-affine deformations of the backbone after uniaxial extension in the nematic phase.[6] This is different from PS chains[9] for which the affinity is lost at high scattering vectors, due to fast relaxation at small scales. In order to refine the comparison, it soon appeared that a better knowledge of the terminal time of PMA−CH_3 chains was necessary, but it could not be found in the literature. Such a determination requires samples of well-defined molecular weight; meanwhile, most of the polymers studied until now have large molecular weight distributions or are shorter than the ones we are studying. This is why we prepared six fractionated samples.

This article reports rheological measurements obtained by oscillatory shear in the isotropic phase for the fractionated samples and in both isotropic and nematic phases for a primary nonfractionated one. The experimental details concerning the polymers and the rheo-

† CEA Saclay.
‡ ULP.
§ Institut Curie.

10.1021/ma9714272 CCC: $15.00
Published on Web 09/30/1998

Table 1. Value of the Weight Average Molecular Weight, M_w, and of the Polydispersity, I_w, of the Samples[a]

M_w	760 000	505 000	265 000	125 000	70 000	40 000	25 000	300 000
	D	D	D	D	H	D	H	H
I_w	1.19	1.19	1.16	1.19	1.26	1.15	1.13	3.91
β (rad)		0.64	0.61	0.62	0.66	0.56	0.54	0.77

[a] They are either deuterated (D) or hydrogenated (H) on the five possible positions of the backbone for SANS use. β indicates the position of the center of the Cole−Cole circle (see Section III). The last column is for the sample of large molecular weight distribution.

logical experiments will be described in section I; results will be given in section II and discussed in section III.

I. Experimental Details

I.1. The Polymers. The hydrogenated or deuterated polymers (for SANS use) were obtained by free radical polymerization of corresponding methacrylate monomers in solution.[10] To reduce their large molecular weight distribution (polydispersity $I_w = M_w/M_n$ greater than 2.5), they were fractionated using a precipitation method with 1,2-dichloroethane as good solvent and methanol as bad solvent.

The samples were analyzed by size exclusion chromatography with small angle light scattering on line (SEC−LS) at the ICS, Strasbourg, France, to obtain the molecular weight distribution, characterized by M_w and I_w. Results are reported in Table 1.

A primary, nonfractionated, sample was also used. Its high polydispersity ($I_w = 3.9$) could mean that the sample is branched. But, then, the ratio M_z/M_w (where M_z is the third moment of the weight distribution) would be very high.[11] This is not the case here, since M_z/M_w equals 3.1.

Differential scanning calorimetry was used to obtain T_g and T_{NI} (temperature of the nematic to isotropic transition). Heating rates were 15 °C/min for T_g determinations and 2 °C/min for T_{NI}. Temperatures of transitions are

$$T_g = 44 \pm 1\ °C$$

$$T_{NI} = 83 \pm 1\ °C$$

T_g is independent of the molecular weight: we checked that, within the full range of molecular weight used here, T_g varied by less than 2 °C, which remains inside the error bars. This can be understood by considering that the smallest molecular weight sample accounts for seventy bulky monomers. Thus, the role of chain ends is negligible, and T_g is not sensitive to it.[12] This is very different from what is encountered with main-chain liquid crystalline polymers, which have no hanging groups and are also shorter ($N < 50$).[13]

The PMA−CH_3 density was estimated at 25 °C by determinations of the volume and weight of molded samples: $\rho = 1.17 \pm 0.03$ g/cm^3.

I.2. Rheological Experiments. The sample with large molecular weight distribution was analyzed at the Ecole des Mines, Sophia-Antipolis, France, in a classical cone−plate apparatus: a Rheometrics (25 mm diameter and 0.1 rad angle) with a frequency range of 10^{-3}−10^1 Hz. The polymer in benzene solution was dried under vacuum at room temperature for at least 48 h. A disk was then molded under vacuum at 130 °C for 12 h at the cone−plate dimension. Linear viscoelastic response was verified at each temperature (71.5, 73.5, 76, 80, 86, 91, 107, 117 °C) and angular frequency, ω (rad/s), by checking that the measured values of storage modulus, $G'(\omega)$, and loss modulus, $G''(\omega)$, were independent of a strain amplitude variation by a factor of 2. The chosen strains were 10% in the isotropic phase and 0.5% in the nematic phase. Between two experiments in the nematic phase, the sample was heated in the isotropic phase (90 °C) while continuously sheared in order to erase any possible orientation.

Due to small amounts of fractionated samples, another device was used for their analyses. It was a piezorheometer (ULP, Strasbourg, France) consisting of two glass slides stuck with two piezoelectric ceramics. One imposes the sine wave displacement, the other measures the transmitted stress.[14] The frequency range was 10^{-1}−10^4 Hz. The powder of dried polymer was put on the preheated lower slide (at 140 °C) and left alone for 1 h in order to expel air bubbles. The thickness of the sample was about 110 μm; thus only 45 mg of product was needed. The two glass slides had been previously scratched perpendicularly to the displacement, using a diamond paste (0.25 μm), in order to limit the sliding of the polymer on the surface. Here again, linearity was verified at each temperature (80, 100, 110, 120, 130, 140 °C). The strains chosen varied from 0.01% to 0.1%. At low temperatures, in the nematic phase, motions became so slow that only the fast region of the relaxation spectrum, the so-called glassy zone, could be observed in the frequency range accessible (limited to 0.1 Hz). Thus, only the isotropic phase was studied with the fractionated samples.

A good overlap of the data insured the consistency of the two experimental sets.

The molecular weight distribution of the different samples was controlled after the rheological measurements. Since it was the same as before the shearing, no degradation (such as chain scission or cross-linking) had occurred.

II. Results

II.1. Time/Temperature Superposition. For the sample with a large dispersion of molecular weight, storage modulus, G', and loss modulus, G'', curves as a function of ω are shown in Figure 1a at three temperatures of the nematic or isotropic phases. These curves can be superposed to the one at $T_0 = 117$ °C, by shifting the data along the frequency axis (Figure 1b). The shift factors, a_{T/T_0}, used are tabulated in Table 2. The same value of a_{T/T_0} can be applied to obtain master curves for the other rheological functions.

The empirical principle of time−temperature superposition is therefore found to hold at all the temperatures probed, allowing master curves to be drawn at the reference temperature T_0. This implies that the time−temperature superposition works across the nematic to isotropic transition for the sample with a large distribution of molecular weight, as previously observed.[3,4]

For the fractionated samples, the same procedure can be applied with data in the isotropic phase. Examples of master curves of $G'(\omega)$ and $G''(\omega)$ are given in Figure 2 for three molecular weights. The shift factors a_{T/T_0}

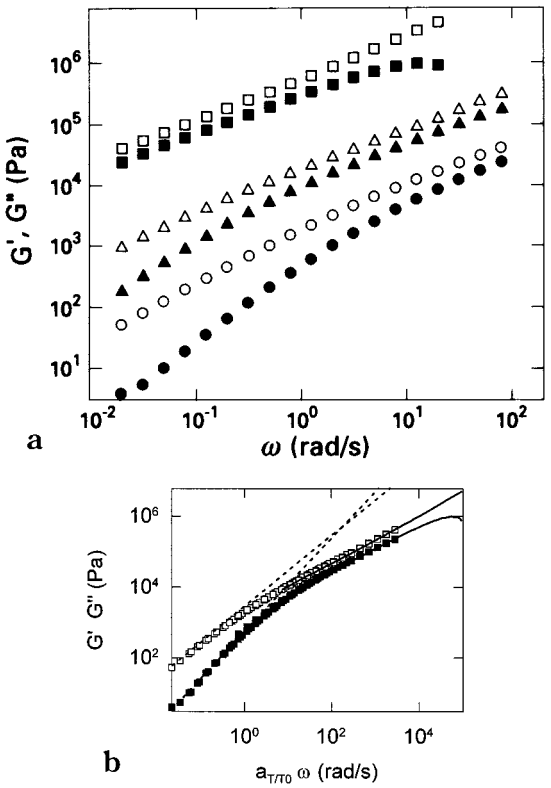

Figure 1. Time-temperature superposition of storage modulus, G', dark symbols, and loss modulus, G'', open symbols, vs angular frequency, ω, for a PMA−CH_3 of molecular weight 300 000 and polydispersity 3.9. (a) Moduli curves for three temperatures: 71.5 °C (■,□), 91 °C (▲,△), and 117 °C (●,○). (b) Master curves at the reference temperature $T_0 = 117$ °C in isotropic phase (symbols) and nematic (solid curves) phase. At low frequencies, data obey classical laws for a viscous liquid: $G' \sim \omega^2$ and $G'' \sim \omega$. These laws are represented by the dashed lines.

Table 2. Time/Temperature Shift Factors, a_{T/T_0}, for Superposition of $G'(\omega)$ and $G''(\omega)$ Curves at Different Temperatures of the Isotropic (I) and Nematic (N) Phases to Curves at the Reference Temperature T_0

nonfractionated sample		fractionated samples	
T (°C)	a_{T/T_0} ($T_0 = 117$ °C)	T (°C)	a_{T/T_0} ($T_0 = 120$ °C)
117 (I)	1	140 (I)	0.18
107 (I)	2.8	130 (I)	0.46
91 (I)	22	120 (I)	1
86 (I)	36	110 (I)	2.8
76 (N)	93	100 (I)	7.9
73.5 (N)	2300		
71.5 (N)	4400		

used are identical irrespective of the value of M_w. This is consistent with the time−temperature superposition principle in that each characteristic time is related to the elementary monomeric one.

The temperature dependence of the shift factors does not obey the WLF equation as for linear polymer but rather obey an Arrhenius law

$$a_{T/T_0} \sim \exp(\Delta H_a/k_B T) \qquad (1)$$

with an activation energy for flow, ΔH_a, of 59 kcal/mol in the nematic phase and 33 kcal/mol in the isotropic phase for the polydispersed sample. For the fractionated samples, the value ΔH_a found in the isotropic phase is slightly different, 29 kcal/mol. These values are

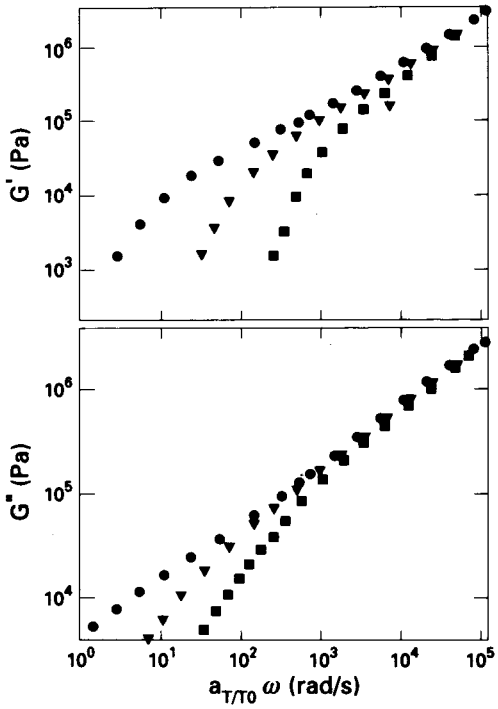

Figure 2. Master curves at $T_0 = 120$ °C of G', upper curve, and G'', lower curve, vs frequency, ω, for three molecular weights: $M_w = 505\,000$ (●), 125 000 (▲), 40 000 (■). For reason of clarity, all the data are not plotted.

rather consistent with those found by other teams (see Table 3) on CLLC polyacrylates, polymethacrylates, or polysiloxanes. Here, the ratio $\Delta H_{a\ nem}/\Delta H_{a\ iso} = 1.8$ is slightly bigger than that found by Colby et al.,[3] 1.6 ± 0.1.

II.2. Molecular Weight between Entanglements. A fundamental point in understanding polymer dynamics is to know whether the chains are entangled or not. This can be inferred from the existence of a rubbery plateau in the $G'(\omega)$ curve. Such a plateau generally appears at frequencies intermediate between fast local movements (at scales lower than the distance between entanglements) and slow ones (at frequencies lower than the inverse terminal time). The average number of monomers between two neighboring entanglements in a chain is N_e, and M_e stands for the corresponding molecular weight.

In this work, the sample with large molecular weight distribution shows no rubbery plateau. This could be due to a large overlap of relaxation times. What is more surprising is that the fractionated samples show no plateau either (see Figure 2a), even with rather large degrees of polymerization. A plateau appears only for the highest molecular weight sample ($M_w = 760\,000$), yet it is not very prominent (Figure 3).

A first estimation of M_e can be obtained from the critical molecular weight M_c. M_c is defined for linear polymers as the crossover value between $\eta_0 \sim M$ and $\eta_0 \sim M^{3.4}$ behaviors.[15] An under-estimated M_c value can be determined in the isotropic phase from the minimum in loss tangent, tan δ, for the sample of highest molecular weight ($M_w = 760\,000$ and $M_n = 640\,000$, where M_n is the number average molecular weight). In this case, an accurate determination of M_c is impossible due to the obvious presence in the sample of chains with M

Table 3. Comparison of the Activation Energy for Flow in the Isotropic, ΔH_a^I, and Nematic, ΔH_a^N, phases for Different CLLC Polyacrylates, Polymethacrylates, or Polysiloxanes

polymer	ΔH_a^N (kcal/mol)	ΔH_a^I (kcal/mol)	$\Delta H_a^N/\Delta H_a^I$
fractionated polymethacrylate[a]		29	
non fractionated polymethacrylate[a]	59	33	1.79
polymethacrylate[3]	38	25	1.51
polyacrylate[3]	33	21	1.57
polymethacrylate[35]	*b*	33	
polymethacrylate[4]	42	25	1.68
polyacrylate[4]	27	16	1.63
polysiloxane $N_w = 95$[36]	23[c]	15[c]	1.52
polysiloxane $N_w = 50$[36]	21[c]	12[c]	1.72

[a] This work. [b] Kannan et al. found the nematic polymer to obey a WLF law. [c] Activation energy obtained from viscosity measurements.

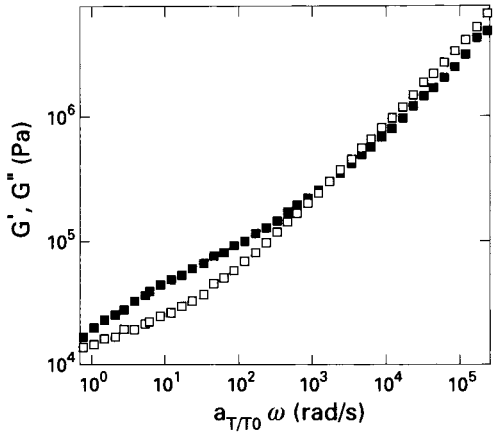

Figure 3. Master curves at $T_0 = 120$ °C of storage modulus, G' (■), and loss modulus, G'' (□), vs frequency, ω, for a PMA−CH_3 sample of molecular weight 760 000 and polydispersity 1.19. The plateau in the $G'(\omega)$ curve is not very marked, but one can note that G'' lies below G' is the corresponding zone. At high frequencies, a frequency power law $G^* \sim \omega^{0.60}$ is obtained.

$< 2M_c$ (see discussion on p 377 in ref 12). Following

$$\tan \delta_m < 1.04(0.75\ M_n/M_c)^{-0.80} \qquad (2)$$

one gets

$$M_c > 225\ 000$$

Since M_c is generally taken as $2M_e$, one obtains

$$M_e > 110\ 000$$

or

$$N_e > 290$$

A second method, based on the calculation proposed by Fetters et al.[16] for random coils, was also used to determine M_e. M_e is the molecular weight of the chain spanning a volume ($\sim R_g^3(M_e)$, where R_g is the chain radius of gyration) in which another chain can be entirely incorporated. This leads to

$$M_e = 4/(A^2\rho^2 N_a^2(\langle R_g^2\rangle/M)^3) \qquad (3)$$

where A is a constant of order unity connecting the volume spanned by the chain to R_g^3, ρ is the bulk density, and N_a is Avogadro's number. R_g of PMA−CH_3 is determined from SANS experiments; we have obtained[8]

$$R_g = 0.143M^{0.5} \qquad (4)$$

which proves the Gaussian character of the chains in the isotropic phase. Taking $\rho = 1.17\ 10^{-24}$ g/Å^3 and $A = 1.59$ at 360 K, eq 3 gives $N_e = 925$ ($M_e = 370\ 000$).

Using this value in the relation

$$G_N^0 = 4\rho RT/5M_e \qquad (5)$$

we estimate a value for the plateau modulus: $G_N^0 = 7.8 \times 10^3$ Pa. This value is about 1 order of magnitude smaller than the one seen in Figure 3! This could mean that a mechanism different from entanglements gives rise to elasticity in the melt.

Such high values of N_e are striking compared to the one known for PS, i.e. about 175 monomers. We would like to insist that this increased N_e value does not come from the backbone rigidity. We have measured the persistence length for PMA−CH_3 and found it roughly equal to the one of PS measured by the same method: $l_p = 10$ Å instead of 9 Å for PS. As remarked by Lin,[17] eq 3 only describes the fact that the volume of one entanglement, $R_g^3(M_e)$, contains a constant number of strands of $N_e b/2l_p$ Kuhn steps ($b = 2.5$ Å is the monomer length). If one describes the Kuhn step as a cylinder of length $2l_p$ and diameter d, then

$$N_e = 200(2l_p)/b(d/(2l_p))^4 \qquad (6)$$

Thus, a large N_e would be related to the thick aspect ratio $2l_p/d$ of comblike chains. With $N_e = 925$, this ratio is about 1.15 (compared to 1.68 for PS) giving a cylinder diameter $d = 17.4$ Å (compared to 11 Å for PS). Since the length of the elongated hanging moieties is 25 Å, this confirms the fact that the six-carbon spacer is very flexible at high temperature (otherwise, the Kuhn step diameter would be 50 Å).

Moreover, the N_e value of 925 is in rather good agreement with those estimated by Rubin et al.[18] for two CLLC polymethacrylates with different terminal groups ($N_e = 660$ and 780).

Thus, we conclude that the samples are not entangled, except for the highest molecular weight ($M_w = 760\ 000$), which is about twice M_e.

II.3. Determination of Terminal Times and Zero Shear Viscosities in the Terminal Zone. For linear polymers, an average terminal time can be estimated by using a Cole−Cole plot, where the imaginary part of the viscosity, $\eta''(\omega) = G'(\omega)/\omega$ is plotted versus its real part, $\eta'(\omega) = G''(\omega)/\omega$. The data can be fitted by a circular arc corresponding to a specific distribution of

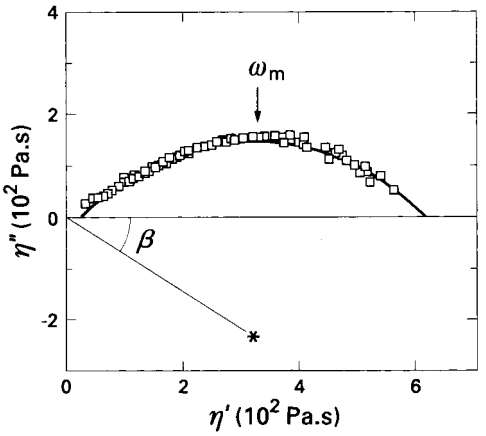

Figure 4. Cole−Cole plot, imaginary viscosity η'' vs real viscosity η', for a PMA−CH_3 of molecular weight 125 000 and polydispersity 1.19 at 120 °C. Data are fitted by a circle (solid curve). The arrow indicates the point where the circle reaches its maximum, giving the frequency ω_m and therefore the average terminal time $\tau_{ter} = 1/\omega_m$. The angle β indicates the position of the circle center and reflects the width of the terminal times distribution.

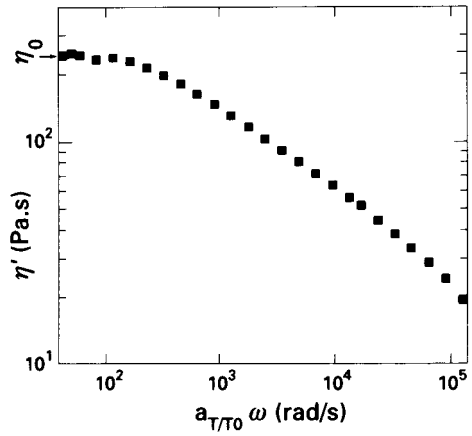

Figure 5. Master curve at $T_0 = 120$ °C of the real part of the complex viscosity, η', vs frequency, ω, for a PMA−CH_3 of M_w = 70 000 and polydispersity $I_w = 1.26$. The plateau at low frequencies allows determination of zero shear viscosity, η_0.

relaxation times.[19] The frequency, ω_m, for which the arc reaches its maximum, gives an average terminal time

$$\tau_{ter} = 1/\omega_m \tag{7}$$

Figure 4 represents the Cole−Cole plot for the M_w = 125 000 fraction. The fit is not very good, due to a peculiar behavior at high frequencies (see next section). Nevertheless, this method is used here, in order to allow a direct comparison with linear polymers. A more conventional determination of a terminal time is to find the intersection point between the two asymptotic variations of G' ($\sim\omega^2$) and G'' ($\sim\omega$) in the terminal zone, as shown in Figure 1b. This method could not be applied to data of samples with highest molecular weights, for which the terminal zone was not large enough. That's why we used the less conventional Cole−Cole method in order to determine the terminal time for all the molecular weights in a consistent way. However, we verified that the terminal times obtained with the two methods were of the same order of magnitude (see Figure 6b).

The limit value of $\eta'(\omega)$ at low frequencies gives the zero shear viscosity, η_0 (Figure 5). Here again, for the highest molecular weights, $\eta'(\omega)$ did not reach a constant value in the frequency range used. η_0 is then obtained from the Cole−Cole plot: it corresponds to the intercept of the arc with the abscissa axis. We verified, for the smallest molecular weights, that the two methods gave values in good agreement. However, the error bars can be larger for the highest molecular weights.

In Figure 6, values of η_0 and τ_{ter} are plotted as a function of M_w, in the isotropic phase (120 °C). These two curves give the following power laws:

$$\eta_0 \sim M_w^{1.3 \pm 0.1} \tag{8a}$$

$$\tau_{ter} \sim M_w^{2.6 \pm 0.3} \tag{8b}$$

These results are not the expected ones. Since chains are not entangled, they should follow a Rouse dynamics

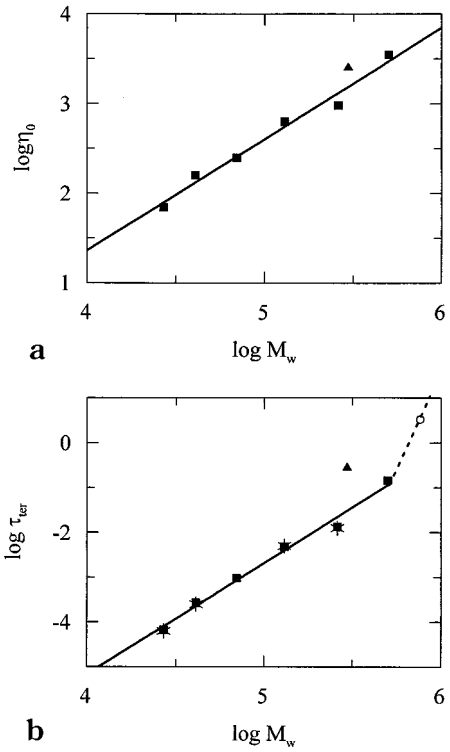

Figure 6. (a) Variation of logarithm of zero shear viscosity, log η_0, as a function of logarithm of weight average molecular weight, log M_w, at 120 °C. Squares correspond to fractionated samples and the triangle to the polydispersed one. (b) Variation of average terminal time, log τ_{ter} as a function of logarithm of weight average molecular weight at 120 °C. Squares correspond to Cole−Cole terminal time of fractionated samples and the triangle to the polydispersed one. The open circle is the minimum value of Cole−Cole terminal time for M_w = 760 000. Stars are terminal times obtained from the intersection of the terminal laws for G' and G'' as explained in Figure 1. Straight lines are two least-squares fits for fractionated samples. Equations of these fits are as follows: $\eta_0 = 2.5 \times 10^{-4}\, M_w^{1.25}$ and $\tau_{ter} = 8.0 \times 10^{-16}\, M_w^{2.5}$ where η_0 is in Pa·s, τ_{ter} in s, and M_w in g/mol.

as for linear polymers; that is to say

$$\eta_0 \sim \zeta_0 M \tag{9a}$$

$$\tau_{ter} \sim \zeta_0 M^2 \tag{9b}$$

where ζ_0 is the monomeric friction coefficient. Let us

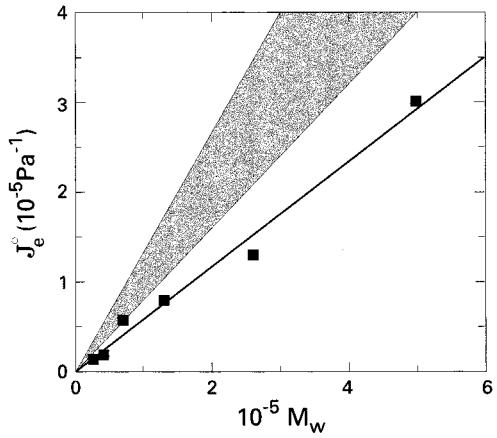

Figure 7. Steady-state compliance, J_0^e, vs weight average molecular weight, M_w at $T_0 = 120$ °C. Experimental data are fitted by a straight line. The expected Rouse variation for linear chains is the shaded sector.

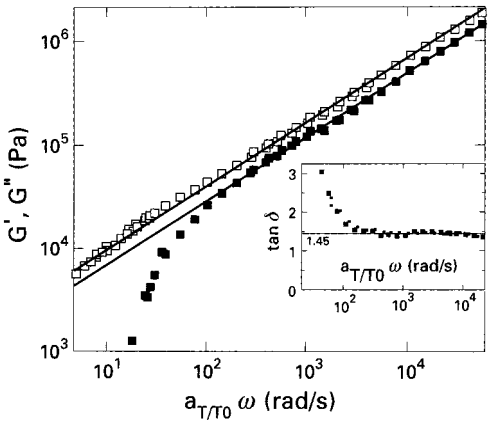

Figure 8. Master curves at $T_0 = 120$ °C of moduli, G' (■) and G'' (□), vs frequency, ω, for the sample of $M_w = 265\,000$ and $I_w = 1.16$. The slope of straight lines is 0.60. The insert gives the variation of loss tangent, tan δ, vs frequency. The 1.45 value leads to $u = \delta^*2/\pi = 0.62$, which shows the result consistency.

note that the effect of chain ends may induce, for small molecular weights, a dependence of ζ_0 with M_w.[12] This is accompanied with a variation of T_g with M_w. The fact that T_g is independent of M_w, as reported in section I, shows that no end effect is relevant here. Equation 9 is therefore quantitatively different from experimental results, eq 8.

For the highest molecular weight ($M_w = 760\,000$), the terminal zone was not accessible at all in the frequency range studied. Nevertheless, one can reasonably assume that the terminal time is greater than the highest accessible time: $1/\omega_{min}$. For this sample, the equivalent value of ω_{min} is 3.10^{-1} rad/s (using time/temperature superposition), so τ_{ter} is greater than 3 s. This lowest value is reported in Figure 6b, where it lies well above the straight line given by eq 8b. Therefore, the average terminal time corresponding to the highest molecular weight must also be well above this line. If we reasonably assume that the reptation regime is reached, we can enclose the M_c value

$$500\,000 < M_c < 760\,000$$

or

$$625 < N_e < 955$$

This range is consistent with $N_e = 925$ estimated from Fetters et al.'s calculation.

In Figure 6, we also report the zero shear viscosity and average terminal time for the nonfractionated sample ($M_w = 300\,000$, $I_w = 3.9$, cone-plate rheometer). On one hand, the η_0 value is consistent with those of fractionated samples. It is not surprising since η_0 is known[20] to depend only on M_w. On the other hand, the value of τ_{ter} is much higher than that of the fractionated sample of same M_w. This is also expected according to the fact that the terminal zone is generally broadened with samples of large molecular weight distribution.

Finally, let us mention another observation in this frequency range concerning the steady-state compliance ($J_0^e = \lim_{\omega\to 0} G'(\omega)/G''(\omega)^2$). In Figure 7, the variation of J_0^e with M_w is linear, as expected for a Rouse dynamics. Let us note that the slope ($J_0^e = 0.2M/\rho RT$) lies outside the limits encountered for a linear polymer free of entanglements and well above T_g:[21]

$$0.3 < J_0^e \rho RT/M < 0.5 \qquad (10)$$

Values of J_0^e lower than the expected ones for linear nonentangled chains mean that the terminal modulus ($1/J_0^e$) is higher than it should be. This can be compared to the anomalous high value of G_N^0.

II.4. The Frequency Power Law of the Transition Zone. Looking at the variation of G' and G'' at intermediate frequencies, we obtained the same power law in both isotropic and nematic phases (Figure 8):

$$G'(\omega) \sim G''(\omega) \sim \omega^u \qquad (11)$$

The exponent u is 0.60 for fractionated samples and 0.65 for the polymolecular one.

Such a departure from the Rouse regime, where the expected exponent is $^1/_2$, has previously been observed[22] for linear polymers: for example, for entangled polybutadiene and PMMA, u is 0.67. However, even if such data exist for a long time, there is still no reasonable explanation for this nonuniversality.[23] This departure from the theoretical Rouse regime is systematically observed with CLLC polymers, whatever the chemical structure of the backbone (polysiloxane, polymethacrylate, or polyacrylate): other teams,[24] obtained similar exponents (varying from 0.60 to 0.80). This is why we will now discuss this exponent with all the phenomena observed with CLLC polymers which seem unusual compared to linear polymers.

III. Discussion

PMA−CH_3 differs from a classical linear polymer in two aspects: it is a liquid crystalline polymer and it is a comblike polymer. The liquid crystalline nature does not lead to any particular dynamics: the viscoelastic behavior of CLLC polymers is very similar in isotropic and nematic phases, except for characteristic times (see the different activation energy) which are larger in the nematic phase. On the contrary, the comblike nature of side-chain polymers reveal some peculiar behaviors discussed now.

First, the samples studied (chains ranging from 65 to 1900 monomers) are not entangled, except for the

largest one. This is probably due to the very large lateral extension of the chains.

Second, the chains, though not entangled, do not follow the classical law for the terminal time. Indeed, $\tau_{ter} \sim M^{2.6}$ (and $\eta_0 \sim M^{1.3}$) instead of $\tau_{ter} \sim M^2$ (and $\eta_0 \sim M$). We will come back to this molecular weight dependence at the end of the discussion.

A third point is the frequency power law at intermediate frequencies, also observed with other CLLC polymers.[3,24] The exponent value of 0.60 is not the one predicted by Rouse ($^1/_2$). This departure from theory is observed for some linear polymers but not explained. Some explanation particular to CLLC polymers can be discussed. Colby et al.[3] first suggested that this might be connected to the large polydispersity of their sample. This argument does not hold anymore because we observed this behavior with polymers of either broad or narrow molecular weight distribution. Another explanation proposed is a hindered relaxation due to nematic ordering (the authors could not compare isotropic and nematic phases, since the former was not investigated). We have made the comparison and have observed the same behavior in the isotropic phase, at temperatures up to 60 °C above T_{NI}. So, an assumption of "nematic hindering" cannot explain the exponent value 0.6.

Now, let us developp a totally different point of view: one can see the power law as the signature of a gel just before the percolation threshold.[14] In such a system, monomers are linked to each other by a chemical bound to give three-dimensional objects, called animals. Due to the fractal nature of animals close to percolation threshold,[25,26] the complex modulus $G^* = G' + iG''$ can be expressed as

$$G^* \sim (i\omega/\omega_0)^u \tag{12}$$

where ω_0 is a cutoff frequency corresponding to the glass transition frequency. This can be rewritten as

$$G^* \sim (\omega/\omega_0)^u(\cos \delta + i \sin \delta) \tag{13a}$$

with

$$\delta = \arctan(G'/G'') = u\pi/2 \tag{13b}$$

At low frequencies, eq 12 is connected to usual variations ($G' \sim \omega^2$ and $G'' \sim \omega$) corresponding to the flow of animals.

The good agreement observed with eq 13 (see Figure 8) prompts us to further the analogy. Since the chains are not chemically branched (as can be seen by SEC−LS), the only possible junctions are reversible bounds between side chains. Such bounds must exist in both nematic and isotropic phases. The main difference with chemical cross-linking of monomers is that, here, the reversible knots have a finite lifetime. The first consequence is that parts of a chain can leave one animal for another one. Therefore, this process can create clusters[27] of limited size. For the same reason, a regular ("terminated") network, i.e., where the length of a strand between two links is roughly constant, may never be obtained. The fractal geometry may therefore be maintained.

This idea of temporary ties junctions between several chains has first been proposed, in a different way, by Gallani et al.[24] and Hilliou.[14] They have measured the moduli of a CLLC polysiloxane in the isotropic phase with the same piezo-rheometer but by varying the gap between the emitting and receiving transducers. For the largest gap (100 μm), the curves look like those reported here. Upon diminishing the gap, a plateau (G' = constant) gradually appears at low frequencies. For the smallest gap (13 μm), G' remains constant for all the frequencies used. This surprising change in behavior has been qualitatively explained in terms of transient elastic clusters of macroscopic size (a few tens of micrometers), floating in a viscous medium. The data have been recently explained qualitatively by an association in parallel of an elastic solid and a viscoelastic liquid.[28] In the framework of this approach, it remains, however, to explain why the elastic clusters would possess a macroscopic size.

The peculiar elastic behavior (i.e. large value of G_N^0) observed in our experiments may have a common origin with these elastic entities which are well separated in space. However, our experiments were performed on 120 μm thick samples, which corresponds to the upper limit explored in ref 24. Since our results with the piezorheometer are similar with those obtained with the classical rheometer (cone−plate with a very large gap), the following discussion refers to samples of infinite thickness.

Two other observations could support the existence of clusters in the melt. The first one is the width of the terminal times distribution. For a single relaxation time, the Cole−Cole plot is a semicircle centered on the x-axis. Otherwise, it is a circular arc, whose center is below the x-axis. The angle β between this center and the x-axis (see Figure 4) is a measure of the width of the terminal times distribution: the bigger β, the broader the distribution. A direct relation can be established between β and the polydispersity,[29] since the latter induces a dispersion of molecular weights and consequently a dispersion of terminal times. We can indeed observe such an effect here (see Table 1). Nevertheless, the striking result is that, even with the sample of smallest polydispersity ($I_w = 1.13$), β remains superior to 0.5 rad. Using some data of Cassagnau[30] on PS samples, we obtained $\beta = 0.30$ rad for a fraction of $I_w = 1.12$. The distribution of terminal times is therefore broader for PMA−CH_3 than for PS of the same polydispersity. This could be interpreted as an effect of temporary stuck chains in the PMA−CH_3 melt.

The second observation supporting the idea of clusters is the measured variation of zero-shear viscosity with molecular weight: $\eta_0 \sim M^{1.3}$. Since η_0 is not proportional to M, this means that the viscosity is not the simple sum of monomeric contributions. Other contributions have to be taken into account, perhaps coming from neighboring temporary linked chains.

Let us now discuss models. Leibler et al.[31] consider entangled linear chains bound by so-called stickers at fixed positions along the chains with a lifetime τ_S. Two stickers are far from each other and separated by several entanglements. Therefore, the dynamics at scales smaller than N_e is not modified by the presence of stickers and remains of Rouse type. In this model, the modulus curve has two plateaus. At short times, both entanglements and stickers are responsible for the first one. It vanishes at $t = \tau_S$. At long times, the second plateau is due to entanglements only. The variation of terminal time is the usual one for reptation ($\tau_{ter} \sim M^{3.4}$). In the case of PMA−CH_3, an interaction between side chains could lead to a sticker. Since each

monomer carries a side chain, the distance between two stickers would be much smaller than N_e. For this reason, Leibler et al.'s model does not apply even for chains long enough to be entangled. On the contrary, the great number of side chains could lead to a distribution of lifetimes instead of a unique τ_S. For example, lifetimes would be different whether a sticker involves two or three or more interacting side chains.

Since PMA−CH_3 chains are mainly nonentangled, it may be more useful to compare our results with Baxandal's predictions.[32] He calculated the self-diffusion coefficient, D, for short chains temporary linked to a network, and predicted a Rouse regime (i.e. $D \sim 1/N$). This result is not in agreement with our observation: we have $D \sim 1/N^{1.6}$ ($R^2 \sim M$, see ref 8, and $\tau_{ter} \sim M^{2.6}$). Let us note that Baxandall considers a *regular* network. This is different from the case of living clusters with a more random structure.

In order to establish a more appropriate theory, one should consider the following questions. One set concerns the stickers: What are their natures, their correlation lengths, their lifetimes? Another set concerns the clusters: What is relationship between the lifetime of a cluster and those of the stickers; do they involve one or several chains? The answers are not trivial since both intra- and interchain stickings exist. As terminal times are increased for a given degree of polymerization compared to a non-entangled linear polymer,[33] we are tempted to say that the movements could be more cooperative and involve several chains.

Another question concerns the dependence of average terminal time with molecular weight, $\tau_{ter} \sim M^{2.6}$. Does τ_{ter} relate to one chain or to one cluster? One thing is clear: if we consider an infinite chain at long times, we must be back to the case of linear chains with $\tau_{ter} \sim M^{3.4}$. There is perhaps a crossover between a regime for small chains, where terminal time relates to the clusters (bigger than a chain), and a regime for long chains, where terminal time relates to the chains themselves.

IV. Conclusion

The viscoelasticity of well-defined comblike liquid crystalline polymers has been investigated by oscillatory shear in isotropic and nematic phases. On one hand, the liquid crystalline nature does not affect the frequency dependence, since the only difference between isotropic and nematic phases is an enhancement of the elementary time. On the other hand, in the isotropic phase, this polymer appears to be different from a linear polymer, probably due to its comblike nature. For example, it shows abnormally high plateau modulus compared to M_e. This leads us to consider the dynamics of living clusters due to stickers between chains (let us note that the above discussion does not presently account for results obtained as a function of sample thickness[24,28]). However, the experimental results in the linear regime may not appear so different from those expected for Rouse chains. We only observe a slight deviation on zero shear viscosity and terminal time. Moreover, the steady-state compliance does vary as M, which is indeed predicted by the Rouse theory. Finally, let us notice that this ambiguity about the Rouse regime is removed by the *nonlinear* behavior observed in high amplitude stretching.[34] Small angle neutron scattering data during the relaxation period following such stretching clearly show that the dynamics is *not* of the Rouse type.

Acknowledgment. V.F.-D., F.B., A.B., J.P.C., and P.K. wish to thank L. Leibler, R. Colby, and M. Daoud for fruitful discussions about theory and interpretation of data and P. Navard, E. Disdier-Peuvrel, and C. Peiti for their help in rheological measurements made at Ecole des Mines, Sophia-Antipolis, France.

References and Notes

(1) See, for instance: *Side Chain Liquid Crystal Polymers*, Mc Ardle, C. B., Ed.; Blackie: London, 1989.
(2) Hsu, C. S. *Prog. Polym. Sci.* **1997**, *22*, 829.
(3) Colby, R. H.; Gillmor, J. R.; Galli, G.; Laus, M.; Ober, C. K.; Hall, E. *Liq. Cryst.* **1996**, *13*, 233.
(4) Zentel, R.; Wu, J. *Makromol. Chem.* **1987**, *187*, 1727.
(5) Marucci, G. in *Liquid Crystallinity in Polymers. Principles and Fundamental Properties*; Ciferri, Ed.; VCH: Weinheim, Germany, 1991.
(6) Brûlet, A.; Boué, F.; Keller, P.; Davidson, P.; Strazielle, C.; Cotton, J. P. *J. Phys. II* (*Fr.*), **1994**, *4*, 1033.
(7) The study of conformation of stretched polymer with neutrons requires quenched samples.
(8) Fourmaux-Demange, V.; Boué, F.; Brûlet, P.; Keller, P.; Cotton, J. P. *Macromolecules*, **1998**, *31*, 801.
(9) Boué, F. *Adv. Polym. Sci.* **1987**, *82*, 48.
(10) Portugall, M.; Ringsdorf, H.; Zentel, R. *Makromol. Chem.* **1982**, *43*, 589.
(11) We have experienced such a situation in the past. We then observed that M_z was very high, corresponding to a tail in the molecular weight distribution for high degrees of polymerization.
(12) Ferry, J. D. *Viscoelastic properties of Polymers*, 3rd ed.; Wiley: New York, 1980.
(13) Sirigu, A. In *Liquid Crystallinity in Polymers. Principles and Fundamental Properties*; Ciferri, Ed.; VCH: Weinheim, Germany, 1991.
(14) Hilliou, L. Thèse de l'Université de Strasbourg, 1996.
(15) Berry, G. C.; Fox, T. G. *Adv. Polym. Sci.* **1968**, *5*, 261.
(16) Fetters, L. J.; Lohse, D. J.; Richter, D.; Witten, T. A.; Zirkel, A. *Macromolecules* **1994**, *27*, 4639.
(17) Lin, Y. H. *Macromolecules* **1987**, *20*, 3080.
(18) Rubin, S. F.; Kannan, R. M.; Kornfield, J. A.; Boeffel, C. *Macromolecules*, **1995**, *28*, 3521.
(19) Cole, K. S.; Cole, R. H. *J. Chem. Phys.* **1941**, *9*, 341.
(20) Masuda, T.; Kitagawa, K.; Inoue, T.; Onogi, S. *Macromolecules* **1970**, *3*, 116.
(21) Graessley, W. W. *Adv. Polym. Sci.* **1982**, *47*, 68.
(22) Tobolsky, A. V. *J. Appl. Phys.* **1956**, *27*, 673.
(23) As noted by one of the reviewers.
(24) Gallani, J. L.; Hilliou, L.; Martinoty, P.; Keller, P. *Phys. Rev. Lett.* **1994**, *72*, 2109.
(25) Daoud, M. *J. Phys.* **1988**, *A21*, L973.
(26) Durand, D.; Delsanti, M.; Adam, M.; Luck, J. M. *Europhys. Lett.* **1987**, *3*, 297.
(27) The term "animal" has a very specific meaning in the frame of polymer gelation theory. That is why, in the following, we would rather use the more generic word "cluster".
(28) Martinoty, F.; Hilliou, L.; Mauzac, M.; Benguigui, L. G.; Collin, D. To be published.
(29) Marin, G. Thèse d'Etat, Pau, 1975.
(30) Cassagnau, P. Thèse de troisième cycle, Pau et Pays de l'Adour, 1988.
(31) Leibler, L.; Rubinstein, M.; Colby, R. H. *Macromolecules* **1991**, *24*, 4701.
(32) Baxandal, L. G. *Macromolecules* **1989**, *22*, 1982.
(33) For instance, at $T_g + 75$ °C, a nonentangled PS of $N = 180$ monomers has a terminal time of about 10^{-4} s, though a PMA−CH_3 of same length has a terminal time of 6×10^{-3} s.
(34) Fourmaux-Demange V. Thèse de l'Université d'Orsay, 1998.
(35) Kannan, R. M.; Kornfield, J. A.; Schwenk, N.; Boeffel, C. *Macromolecules* **1993**, *26*, 2050.
(36) Fabre, P.; Veyssié, M. *Mol. Cryst. Liq. Cryst. Lett.* **1987**, *4*, 99.

MA9714272